Bayesian Non-Parametric Frailty Model for Dependent Competing Risks in a Repairable Systems Framework

Marco Pollo Almeida[12], Rafael Paixão[12], Pedro L. Ramos[2*], Vera Tomazella[1], Francisco Louzada [2], Ricardo S. Ehlers[2]

[1] *Federal University of São Carlos, São Carlos, São Paulo, Brazil*

[2] *Institute of Mathematical and Computer Sciences, University of São Paulo, São Carlos, São Paulo, Brazil*

Abstract

The aim of this article is to analyze multiple repairable systems data under the presence of dependent competing risks. It is known that the dependence effect in this scenario influences the estimates of the model parameters. Hence, under the assumption that the cause-specific intensities follow a power law process (PLP), we propose a frailty-induced dependence approach to incorporate the dependence among the cause-specific recurrent processes. Moreover, the misspecification of the frailty distribution may lead to errors when estimating the parameters of interest. Because of this, we considered a nonparametric approach to model the frailty density using a Dirichlet process mixture prior, which offers more flexibility to provide consistent estimates for the PLP model, as well as insights about heterogeneity among the systems. We proposed an orthogonal parametrization for the PLP model parameters that allowed us to specify a joint prior distribution for the parameters that returned closed-form estimators for the posterior mean. Additionally, a hybrid MCMC sampler algorithm composed by Hamiltonian Monte Carlo and Gibbs sampling was built for computing the posterior estimates with respect to the frailty distribution. A simulation study was conducted to evaluate the efficiency of our estimates. This method was used to analyze a real dataset. Algorithms, code, and data are provided in supplementary material available online.

Keywords: bayesian non-parametric, shared frailty, repairable systems, power law process, dependent competing risks, Hamiltonian Monte Carlo.

1. Introduction

Studying recurrent event data is important in many areas such as engineering, social and political sciences and in the public health setting. For example, in the engineering, failure of a mechanical or electrical component may occur more than once; the recurrence of bugs over time in a software system that is under development. In particular, in reliability analysis, interest is usually centered on failure data from complex repairable systems. Monitoring the status of a repairable system leads to a recurrent events framework, where events correspond to failures of a system.

The primary challenge when modeling repairable systems data is how to account for the effect of a repair action performed immediately after a failure. The most explored assumptions are either minimal repair and perfect repair. In the former, it is supposed that the repair action, after a failure, returns the system to the exact condition it was immediately before it failed and is enough to make the system operational again. In the latter, the repair action leaves the system as if it were new.

The failure history of a repairable system, under a minimal repair strategy, is usually modeled according to a nonhomogeneous Poisson process (NHPP). In the repairable system literature, one of the most important and well-known parametric forms for the NHPP model is the power law process (PLP). We emphasize an alternative specification of the PLP, which is obtained by using a simple operational definition of its parameters, making them orthogonal to each other. The model we discuss here is based on such reparametrization because it results in mathematical and computational simplifications for our research.

Recently, in the statistical and engineering literature, there has been increasing interest in examining failure data of systems that are subject to multiple recurrent causes of failures. This setting may be expressed as a series system where components are connected in series, in such a way that the failure of a single component results in system failure. The same setting may be expressed in an alternative way by a repairable system in which components can perform different operations, and thus be subject to different types of failures. Traditionally, models with this characteristic are known as competing risks. In complex systems, such as supercomputers, aircraft generators, industrial plants, jet engines, and cars, the presence of multiple types (or causes) of failure is common. From an economic perspective, such systems are commonly repaired rather than replacing the system with a new one after failure.

Of particular concern is dealing with multicomponent systems when there is stochastic dependency among components. It means that the condition of a component influences or induces the failure of other components and vice-versa. We can call this case dependent competing risks. It is important to point out that neglecting existing dependence can lead to estimation

errors and bad predictions of system behavior. A number of authors have considered the effects of dependence and several approaches have been discussed in the literature [1; 2; 3; 4; 5; 6].

In this paper we propose a model for multiple identical repairable systems under the action of dependent competing risks, using non-parametric frailty that takes into account a flexible class of distributions. The reasoning of our approach is to apply a Bayesian nonparametric prior, i.e. the Dirichlet process mixture (DPM), to describing uncertainty in the distribution of frailty and also due to their flexibility in modeling unknown distributions, in order to avoid making incorrect specifications. Although this model has infinite parameters, due to the infinite mixture model, it is a flexible mixture, parsimonious, and simple to sample. We chose the stick-breaking representation of the Dirichlet process prior [7], because of a simple implementation to build the algorithm. To obtain the posterior distribution, we created a hybrid MCMC algorithm [8], using the Gibbs sampler [9] and the Hamiltonian Monte Carlo (HMC) method [10]. It is important to point out that, no studies have been found which explore the use of DPM for frailty density in the context of multiple repairable systems under the action of dependent competing risks. Regarding PLP parameters, we propose a class of noninformative priors whose resulting posterior distributions are proper and we obtained closed-form Bayesian estimators. It is also worth mentioning that one of the motivating arguments of the article is in the context of manufacturing and industrial processes, specifically, where improvement in the reliability of a repairable system is an important factor in developmental testing programs whose inferential methodology of reliability growth curves plays a key role in the iterative process of testing, identifying failures, analyzing their causes, finding solutions, improving design, and implementing them in the prototypes being tested, see for instance, [11; 12], and the references therein.

The remaining part of the paper proceed as follows: In Section 2, fundamental groundwork in terms of repairable systems, dependent competing risks and shared frailty model is presented. The Bayesian analysis is developed in Section 3, with a discussion on the choice of priors distributions for the proposed model and the computation of posterior distributions. In Section 4, an extensive simulation study is described in order to evaluate the efficiency of the proposed Bayesian estimators, and Section 5 uses them to analyze a real data set that comprises the failure history for a fleet of cars under warranty. Section 6 concludes the paper with final remarks.

2. Background

In this section, we present a theoretical background in order to provide groundwork for the development of the proposed model. Hereafter, random variables are denoted by capital letters (e.g. Z_j, N_{jq}), while their realizations are denoted by the lowercase (e.g., z_j, n_{jq}).

2.1. Multiple repairable systems

Here, we present a brief overview to analyze data from multiple repairable systems. We highlight just two important assumptions in this context. The first is to assume that all systems are identical or different. The second is to assume that all systems have the same truncation time τ or, otherwise, have different truncations at τ_j. However, for the sake of simplicity and brevity of exposition, we assumed the observation lengths, τ, for each system to be equal. Moreover, in this paper, we assume all systems to be identical, i.e., the systems are specified as m independent realizations of the same process, with intensity function λ.

If the multivariate counting processes $N_1(t), \ldots, N_m(t)$ are all observed at the same time τ, the NHPP resulting from the superposition of NHPPs is given by $N(t) = \sum_{j=1}^{m} N_j(t)$ and has an intensity function given by $\lambda(t) = m\lambda(t)$; e.g., overlapping realizations of a PLP. Therefore, inferences in models proposed for this framework can be made through the following likelihood function

$$L(\lambda) = \left(\prod_{j=1}^{m}\prod_{i=1}^{n_j} \lambda(t_{ji})\right) \exp\left(-\sum_{j=1}^{m}\int_0^{\tau} \lambda(s)ds\right).$$

The m systems are considered to be identical, and therefore have the same intensity function and thus we would have a random sample of systems. On the other hand, this assumption may not be true. That is, in many real-world reliability applications there may be some heterogeneity between "apparently identical" repairable systems. In this case, it is necessary to propose a statistical model capable of capturing this heterogeneity (see [13]). [14; 15] discuss frailty models for modeling and analyzing repairable systems data with unobserved heterogeneity.

2.2. Recurrent Competing Risks Model for a Single Repairable System

To achieve understanding, we start this section by assuming a single competing risks system with K components under observation during the interval $(0, T]$ (time-truncated case), alternatively, a repairable system in which components can perform different operations, and thus be subject to K different types of failures.

At each failure, the cause of failure (or failure mode) is denoted by $\delta(t_i) = \delta_i = q$ for $q = 1, 2, \ldots, K$. If n failures have been observed in $(0, T]$, then we observe the data $(t_1, \delta_1), \ldots, (t_n, \delta_n)$, where $0 < t_1 < \cdots < t_n < T$ are the system failure times and the δ_is represent the q-th associated failure cause with i-th failure time for $i = 1, \ldots, n$. Let $N(T) = n$ be the number of observed failures in $(0, T]$. Suppose a process $\{N(t); t \geq 0\}$ having independent increments and starting at $N(0) = 0$ is defined to be a Poisson process with intensity function $\lambda(t)$ if, for any t, the random variate $N(t)$ follows a Poisson distribution with mean $\Lambda(t) = \int_0^t \lambda(u)du = \mathbb{E}[N(t)]$. In this case, $\{N(t); t \geq 0\}$ is the so-called NHPP. Now, one can introduce a counting process $\{N_q(t); t \geq 0\}$ whose behavior is associated with the cause-specific intensity function

$$\lambda_q(t) = \lim_{\Delta t \to 0} \frac{P(\delta(t) = q, N(t + \Delta t] - N(t) = 1 | N(s), 0 \leq s \leq t)}{\Delta t}.$$

Hence, the cumulative number of failures of the system, $N(t) = \sum_{q=1}^{K} N_q(t)$, is a superposition of NHPPs and its intensity is $\lambda(t) = \sum_{q=1}^{K} \lambda_q(t)$.

Under minimal repair, the failure history of a repairable system is modeled as an NHPP. We give special attention to functional form for the cause-specific intensity according to the PLP. In particular, the PLP provides a flexible parametric form for the intensity of the process given by

$$\lambda_q(t) = \frac{\beta_q}{\psi_q}\left(\frac{t}{\psi_q}\right)^{\beta_q-1}, \tag{1}$$

with $t \geq 0$, $\psi_q > 0, \beta_q > 0$ and for $q = 1, \ldots, K$. The model is quite flexible because it can accommodate both decay ($\beta_q < 1$) and growth ($\beta_q > 1$) in reliability. The corresponding mean function considering time-truncated scenario is

$$\Lambda_q(T) = \mathbb{E}[N_q(T)] = \int_0^T \lambda_q(s)ds = \left(\frac{T}{\psi_q}\right)^{\beta_q}. \tag{2}$$

If we reparametrize (1) in terms of β_q and α_q, where the latter is given by

$$\alpha_q = \left(\frac{T}{\psi_q}\right)^{\beta_q}, \tag{3}$$

one obtain the following advantageous likelihood function

$$\begin{aligned} L(\boldsymbol{\theta}|\boldsymbol{t},\boldsymbol{\delta}) &= \left\{\prod_{i=1}^{n}\prod_{q=1}^{K}\left[\beta_q\alpha_q t_i^{\beta_q-1}T^{-\beta_q}\right]^{\mathbb{I}(\delta_i=q)}\right\}\exp\left\{\sum_{q=1}^{K}\alpha_q\right\} \\ &\propto \prod_{q=1}^{K}\gamma(\beta_q|n_q+1, n_q/\hat{\beta}_q)\prod_{q=1}^{K}\gamma(\alpha_q|n_q+1,1), \end{aligned} \tag{4}$$

where $n = \sum_{q=1}^{K} n_q$; $n_q = \sum_{i=1}^{n}\mathbb{I}(\delta_i = q)$; $\boldsymbol{\theta} = (\boldsymbol{\beta}, \boldsymbol{\alpha})$ with $\boldsymbol{\beta} = (\beta_1, \ldots, \beta_K)$ and $\boldsymbol{\alpha} = (\alpha_1, \ldots, \alpha_K)$; $\hat{\beta}_q = n_q/\sum_{i=1}^{n_q}\log(T/t_i)$ and $\gamma(x|a,b) = b^a x^{a-1}e^{-bx}/\Gamma(a)(x, a, b > 0)$ is the probability density function of the gamma distribution with shape and scale parameters a and b, respectively. It is important to point out that β_q and α_q are orthogonal parameters. For the advantages of having orthogonal parameters, see [16].

2.3. Multiple Repairable Systems Subject to Multiple Causes of Failure

We now turn to the framework for multiple repairable systems and highlight the used notations in the multivariate counting process context. Consider a sample of m identical systems in which each system is under the action of K different types of recurrent causes of failure. Let $N_{jq}(t) = \sum_{i=1}^{n_j}\mathbb{I}(\delta_{ji} = q)$ be the cumulative number of type q failures occurring over the interval $[0, t]$ for the j-th system ($j = 1, \ldots, m$; $q = 1, \ldots, K$ and $i = 1, 2, \ldots, n_j$) where $\{N_{jq}(t), t > 0\}$ is a counting process. Note that $N_{j\bullet}(t) = \sum_{q=1}^{K} N_{jq}(t)$ represents the cumulative number of failures of system j taking into account all failures arising from all components from the j-th system. Let $N_{\bullet q}(t) = \sum_{j=1}^{m} N_{jq}(t)$ denote the number of failures of cause q for all systems. We consider that each system is under observation for all types of events over the same period of time, i.e., $[0, T]$. Thus, let t_{ji}, $i = 1, 2, \ldots, n_j$ be the observed failure times for system j, satisfying $0 < t_{j1} < t_{j2} < \cdots < t_{jn_j} < T$. Besides, denote that $\delta_{ji} = q$ is the failure mode (or component) that caused the system failure. Hence, the observed data is $D_j = \{(t_{ji}, \delta_{ji} = q), i = 1, 2, \ldots, n_j; q = 1, \ldots, K\}$. The complete data is given by $\boldsymbol{D} = (D_1, \ldots, D_m)$. The dataset should be structured as Table 5 in Appendix B.

As mentioned earlier, our focus is mainly on the component level failure process conforms to a PLP, therefore the cause-specific intensity function that governs the counting process $N_{\bullet q}(T)$, taking into to account a orthogonal parametrization in terms of α_q and β_q, is defined as

$$\lambda_q(\boldsymbol{t},\boldsymbol{\delta}) = \beta_q\alpha_q t_{ji}^{\beta_q-1}T^{-\beta_q},\ q = 1, \ldots, K, \tag{5}$$

where α_q is the mean function given by

$$\alpha_q = \mathbb{E}\left[N_{\bullet q}(T)\right] = \Lambda_q(T) = \int_0^T \lambda_q(s)ds. \tag{6}$$

2.4. Frailty-induced dependence approach

This section provides a brief review of the shared frailty model. In addition, we will extend the model (1) presented in the previous section to deal with multiple repairable systems under competing risks in which their cause-specific intensities are subject to a latent (unobserved) random variable, Z_j, for $j = 1, \ldots, m$, that is supposed to act multiplicatively on the referred intensities. For more details on general frailty theory, see [17]; additional results on frailty in the counting process context are given in [18].

In the reliability field, the frailty model is commonly used to model heterogeneous repairable systems [19; 20; 21]. We start to formulate the shared frailty model using a counting process framework and we focus on understanding intensity processes dependent on a frailty term. Suppose that m clusters (or systems) are under observation, where each cluster is composed by K units (or components). The intensity function of the j-th cluster ($j = 1, \ldots, m$) of a shared frailty model is that of the Cox model multiplied by a frailty term Z_j (multiplicative random effect model). More specifically, for each individual counting process, $N_{j\bullet}(t)$, their intensity function conditionally on the frailty Z_j, is given by

$$\lambda_j(\boldsymbol{t},\boldsymbol{\delta} \mid Z_j) = Z_j\lambda(t), \tag{7}$$

where $\lambda(t)$ is the basic intensity function and $j = 1, 2, \ldots, m$. The intensity function (7) describes the recurrent failure process on the j-th cluster and the intensity associated to the q-th component from the j-th cluster is defined as

$$\lambda_{jq}(\boldsymbol{t},\boldsymbol{\delta} \mid Z_j) = Z_j\lambda_q(t), \tag{8}$$

where $\lambda_q(t)$ is the basic intensity function from the q-th component and $q = 1, 2, \ldots, K$. Note that intensities (7) and (8) follow the relation $\lambda(t) = \sum_{q=1}^{K}\lambda_q(t)$ [18]. Henceforth, we will omit the subscript j from λ_{jq} in (8) since we are assuming that the systems are identical, so $\lambda_q(\boldsymbol{t},\boldsymbol{\delta} \mid Z_j) = Z_j\lambda_q'(t)$. Note also that $\lambda_q'(t)$ is referred to as the (basic) intensity function for type q events (e.g., PLP). Let $\boldsymbol{Z} = (Z_1, \ldots, Z_m)$ denote the multivariate random effect, which we assume arises from density $f_Z(\cdot)$,

where each Z_j is independent and identically distributed (iid). These are typically parametrized so that both $E(\boldsymbol{Z}) = 1$ and $Var(\boldsymbol{Z}) = \eta$ are finite, for $j = 1, 2, ..., m$. It is worth pointing out that the Z_js are assumed to be stochastically independent of the failure process $\lambda_q^{'}(t)$ [18; 1].

2.4.1. The shared frailty model for the power law process

Following the previous section, we specify the model (8) in terms of (5) in order to present the likelihood function with a special form. To achieve this purpose, suppose a minimal repair is undertaken at each failure, thus the NHPP is the model of choice. Specifically, the failures from each component follow an NHPP, with PLP intensity function given in (5). Furthermore, let us consider that a realization $z_j \sim f_Z$ acts on all the cause-specific intensities (8) belonging to the j-th system. Thus, conditioning on the frailty term, the model is expressed as

$$\lambda_q(\boldsymbol{t}, \boldsymbol{\delta}|Z_j) = Z_j \beta_q \alpha_q t_{ji}^{\beta_q - 1} T^{-\beta_q} \tag{9}$$

and the mean function is given by

$$\Lambda_q(T|Z_j) = Z_j \alpha_q. \tag{10}$$

Following the arguments of [14; 15], our analysis relies on the constraint $\bar{\boldsymbol{Z}} = \frac{1}{m}\sum_{j=1}^{m} Z_j = 1$, for the sake of identifiability and interpretability. Based on this, we can now construct the likelihood function with the following clear advantage.

2.4.2. Likelihood function

To simplify notation in this section we will drop the subscript $\bullet$ and refer to $n_{j\bullet}$ and $n_{\bullet q}$ as n_j and n_q, respectively. The likelihood contribution from the j-th system based on (9) is given by

$$L_j(\boldsymbol{\theta}, Z_j|\boldsymbol{D}) = \left[\prod_{i=1}^{n_j}\prod_{q=1}^{K}[\lambda_q(\boldsymbol{t}, \boldsymbol{\delta}|Z_j)]^{\mathbb{I}(\delta_{ji}=q)}\right]\exp\left[-\sum_{q=1}^{K}\Lambda_q(T|Z_j)\right], \tag{11}$$

where $\mathbb{I}(\delta_{ji} = q)$ represents an indicator function, $\boldsymbol{\theta} = (\boldsymbol{\beta}, \boldsymbol{\alpha})$ with $\boldsymbol{\beta} = (\beta_1, \ldots, \beta_K)$, $\boldsymbol{\alpha} = (\alpha_1, \ldots, \alpha_K)$ and $\boldsymbol{D} = (D_1, D_2, ..., D_m)$ represents the complete data for $i = 1, \ldots, n_j$; $j = 1, \ldots, m$ and $q = 1, \ldots, K$. Thus, the overall likelihood function is represented by

$$\begin{aligned} L(\boldsymbol{\theta}, \boldsymbol{Z} \mid \boldsymbol{D}) &= \prod_{j=1}^{m} L_j(\boldsymbol{\theta}, Z_j|\boldsymbol{D}) \\ &= c\prod_{j=1}^{m} Z_j^{n_j}\prod_{q=1}^{K}\left[\beta_q^{n_{jq}}\alpha_q^{n_{jq}\beta_q}T^{-n_{jq}\beta_q}\prod_{i=1}^{n_{jq}}\left(t_{ji}^{\beta_q}\right)\right]\exp\left[-Z_j\sum_{q=1}^{K}\alpha_q\right] \\ &\propto \prod_{j=1}^{m} Z_j^{n_j}\prod_{q=1}^{K}\gamma(\beta_q \mid n_q + 1, n_q\hat{\beta}_q^{-1})\gamma(\alpha_q \mid n_q + 1, m), \end{aligned} \tag{12}$$

where $n_j = \sum_{q=1}^{K} n_{jq}$; $n_q = \sum_{j=1}^{m} n_{jq}$; $\prod_{i=1}^{n_{jq}}(\cdot) = \prod_{i=1}^{n_j}(\cdot)^{\mathbb{I}(\delta_{ji}=q)}$; $c = \prod_{j=1}^{m}\prod_{i=1}^{n_{jq}} t_{ji}^{-1}$ and $\gamma(x|a, b) = b^a x^{a-1} e^{-bx}/\Gamma(a)(x, a, b > 0)$ is the probability density function of the gamma distribution with shape and scale parameters a and b, respectively. In addition,

$$\hat{\beta}_q = n_q / \sum_{j=1}^{m}\sum_{i=1}^{n_{jq}} \log(T/t_{ji}), \tag{13}$$

is the MLE for β_q.

As indicated previously, the overall likelihood function (12) may be factored as a product of three quantities, and it is given by,

$$L(\boldsymbol{\theta}, \boldsymbol{Z} \mid \boldsymbol{D}) = L_1(\boldsymbol{Z} \mid \mathbf{D})L_2(\boldsymbol{\beta} \mid \mathbf{D})L_3(\boldsymbol{\alpha} \mid \mathbf{D}), \tag{14}$$

where $L_1(\boldsymbol{Z} \mid \mathbf{D}) = \prod_{j=1}^{m} Z_j^{n_j}$; $L_2(\boldsymbol{\beta} \mid \mathbf{D}) = \prod_{q=1}^{k}\gamma(\beta_q \mid n_q + 1, n_q\hat{\beta}_q^{-1})$ and $L_3(\boldsymbol{\alpha} \mid \mathbf{D}) = \prod_{q=1}^{k}\gamma(\alpha_q \mid n_q + 1, m)$ and it will be used later in our posterior analysis.

3. Bayesian analysis

This section, in turn, is divided into two parts. In the first, we present the choice of the prior distributions for β_q and α_q $(q = 1, \ldots, K)$ in the PLP model. In this case, we consider a similar approach according to the study of Bar-Lev et al. [22]. In the second, we discuss a Bayesian nonparametric approach to model the uncertainty about the distribution of shared frailty. As we will see in this section, we can carry out an individual posterior analysis of the quantities of interest due to the orthogonality among α_q and β_q and the assumption that Z_js are stochastically independent of the failure processes λ_qs.

3.1. Prior specification for α and β

Selecting an adequate prior distribution using formal rules has been widely discussed in the literature [23]. In the repairable systems context, Bar-Lev et al. [22] considered the following class of prior for the PLP model

$$\pi(\alpha, \beta) \propto \alpha^{-1}\beta^{-\zeta}, \tag{15}$$

where $\zeta > 0$ is a known hyperparameter. Following these authors, we apply their main results in the setting of repairable systems under competing risks using the particular parametric formulation of PLP (9). Thus, we propose the prior distribution for the referred context as follows:

$$\pi(\boldsymbol{\alpha}, \boldsymbol{\beta}) \propto \prod_{q=1}^{K}\alpha_q^{-1}\beta_q^{-\zeta}. \tag{16}$$

This class of prior distributions includes the invariant Jeffreys' prior when $\zeta = 1$. Moreover, it reduces to (15) when $q = 1$. Further, we will discuss the chosen value for ζ, and necessary conditions for the obtained posterior to be proper.

Note that, due to (14) and the assumption that Z_js are stochastically independent of the failure processes λ_qs, the joint posterior distribution of (16) is proper. Note also that, the marginal distributions $\pi(\boldsymbol{\beta} \mid \mathbf{D})$ and $\pi(\boldsymbol{\alpha} \mid \mathbf{D})$ are proper since they are independent, as follows:

$$\pi(\boldsymbol{\beta} \mid \mathbf{D}) = \prod_{q=1}^{k}\gamma\left(\beta_q \mid n_q + 1 - \zeta, n_q\hat{\beta}_q^{-1}\right) \tag{17}$$

and

$$\pi(\boldsymbol{\alpha} \mid \mathbf{D}) = \prod_{q=1}^{k} \gamma(\alpha_q \mid n_q, m). \tag{18}$$

Since $\pi(\boldsymbol{\alpha} \mid \mathbf{D})$ is the product of independent gamma distributions, then the marginal joint distribution $\pi(\boldsymbol{\alpha} \mid \mathbf{D})$ is proper. Using the same idea, $\pi(\boldsymbol{\beta} \mid \mathbf{D})$ is the product of independent gamma distributions if $n_q > \zeta$ and, therefore, is a proper marginal posterior distribution.

This work adopts the quadratic loss function, hence the Bayes estimator is the posterior mean which has optimality under Kullback-Leibler divergence. It is worth pointing out that, in this section, the notation adopted for posterior mean will be $\hat{\alpha}_q^{Bayes}$ and $\hat{\beta}_q^{Bayes}$. Therefore,

$$\begin{aligned} \hat{\alpha}_q^{Bayes} &= \mathbb{E}(\alpha_q \mid \mathbf{D}) = \frac{n_q}{m} \\ \hat{\beta}_q^{Bayes} &= \mathbb{E}(\beta_q \mid \mathbf{D}) = \frac{(n_q + 1 - \zeta)}{n_q}\hat{\beta}_q. \end{aligned} \tag{19}$$

Besides the good properties mentioned above, we have that

$$\begin{aligned} &\mathbb{E}\left[\hat{\alpha}_q^{Bayes}\right] = \alpha_q \text{ and} \\ &\mathbb{E}\left[\hat{\beta}_q^{Bayes}\right] = \mathbb{E}\left[\frac{(n_q + 1 - \zeta)}{n_q}\hat{\beta}_q\right] = \beta_q \quad \text{if} \quad \zeta = 2. \end{aligned} \tag{20}$$

Therefore, assuming that $\zeta = 2$ we have that both $\hat{\alpha}_q^{Bayes}$ and $\hat{\beta}_q^{Bayes}$ are unbiased estimators for α_q and β_q. It is worth mentioning that from (20) we observe that the MLE for β_q given in (13) is biased, while the Bayes estimators are unbiased in terms of the posterior mean.

3.2. Bayesian nonparametric approach for frailty distribution

This work presents the frailty distribution as an unknown distribution, therefore we will apply the Bayesian nonparametric methodology. Traditionally, the key idea of the Bayesian nonparametric approach is to obtain inference on an unknown distribution function using process priors on the spaces of densities. According to a definition provided by Sethuraman [7], the nonparametric Bayesian model involves infinitely many parameters. To better understand the technical definition of Bayesian nonparametric models in a broad way, please see [24], [25], for example. There are many methods that specify more flexible density such as finite mixtures, DP, DPM, and mixture of Polya trees. Here, we considered DPM for logarithm of the frailty $\mathbf{W} = \log(\mathbf{Z})$, represented by

$$\begin{aligned} W_1, \ldots, W_m &\sim F \\ F &\sim \mathcal{D}(c, F_0), \end{aligned} \tag{21}$$

where $\mathcal{D}$ is the DP prior with base distribution F_0; c is the concentration parameter and $\mathbf{W} = (W_1, \ldots, W_m)'$. c can also be interpreted as a precision parameter that indicates how close the F distribution is to the base distribution F_0 [26].

Using the stick-breaking representation discussed in Sethuraman [7], a DPM of Gaussian distribution can be represented as infinite mixtures of Gaussian, which is an extension of the finite mixture model. Therefore, a density function of W can be represented by

$$f_W(W) = f_W(W \mid \boldsymbol{\Omega}) = \sum_{l=1}^{\infty} \rho_l \mathcal{N}(w \mid \mu_l, \tau_l^{-1}), \tag{22}$$

where $\mathcal{N}(\cdot \mid \mu, \tau^{-1})$ denotes a normal density function with parameters (μ, τ^{-1}); $\boldsymbol{\Omega} = \{\boldsymbol{\rho}, \boldsymbol{\mu}, \boldsymbol{\tau}\}$ is the infinite-dimensional parameter vector describing the mixture distribution for W; $\boldsymbol{\rho} = \{\rho_l\}_{l=1}^{\infty}$ represents the vector of weights, $\boldsymbol{\mu} = \{\mu_l\}_{l=1}^{\infty}$ is the vector of means and $\boldsymbol{\tau} = \{\tau_l\}_{l=1}^{\infty}$ is the vector of precision, for $l = 1, 2, \ldots$. Note that the density function of Z can be calculated as follows:

$$f_Z(Z) = f_Z(Z \mid \boldsymbol{\Omega}) \quad = \quad \sum_{l=1}^{\infty} \rho_l \mathcal{LN}(z \mid \mu_l, \tau_l^{-1}), \tag{23}$$

where $\mathcal{LN}(\cdot \mid \mu, \tau^{-1})$ denotes log-normal density functions with parameters μ and τ^{-1}. Therefore, Z can be represented as the infinite mixture log-normal. Note that the base distributions of Z and W are a log-normal and a normal distribution, respectively.

Prior specification for Ω

As shown before, $\boldsymbol{\Omega}$ represents a collection of all unknown parameters in (22) and (23). Based on this, we specified a prior distribution for $\boldsymbol{\Omega}$ as follows. Firstly, we specify a prior for $\boldsymbol{\rho}$.

Using the stick-breaking representation for prior distribution of $\boldsymbol{\rho}$, denoted by $\pi(\boldsymbol{\rho})$, parameter vector $\boldsymbol{\rho}$ is reparameterized as follows:

$$\begin{aligned} \rho_1 &= \nu_1, \\ \rho_l &= \prod_{o=1}^{l-1}(1 - \nu_o)\nu_l, \ \forall\, o = 2, 3, \ldots, \end{aligned} \tag{24}$$

where the prior distribution of the vector $\boldsymbol{\nu} = \{\nu_l\}_{l=1}^{\infty}$ is independent and identically distributed with beta distribution denoted by

$$\boldsymbol{\nu} \sim \mathcal{B}(1, c), \tag{25}$$

and the hyper-prior distribution of c is

$$\pi(c) \sim \mathcal{G}(ac_0, bc_0), \tag{26}$$

where $\mathcal{G}(\cdot, \cdot)$ represents the gamma distribution [26]. Besides, we chose a normal-gamma distribution as the prior of $(\mu_l, \tau_l) \sim \mathcal{NG}(m_0, s_0, d_0 p_0, d_0)$, for $l = 1, 2, \ldots$, due to the fact that this prior is conjugate to the normal distribution, where

$$\begin{aligned} &\mu_l \mid \tau_l \sim \mathcal{N}(m_0, (s_0\tau_l)^{-1}), \\ &\tau_l \sim \mathcal{G}(d_0, d_0 p_0). \end{aligned}$$

Thus, joint prior density of $\boldsymbol{\Omega}$ can be expressed as

$$\pi(\boldsymbol{\Omega}) = \pi(c)\pi(\boldsymbol{\rho})\pi(\boldsymbol{\mu}, \boldsymbol{\tau}). \tag{27}$$

For our Bayesian estimation scheme, the joint posterior distribution of $\mathbf{Z}$ and all the unknown parameters in $\boldsymbol{\Omega}$ are reached by joining all the prior information (23), (27) and the likelihood function (14), as follows:

$$\pi(\mathbf{Z}, \boldsymbol{\Omega} \mid \mathbf{D}) \propto L_1(\mathbf{Z}|\mathbf{D}) f_Z(\mathbf{Z} \mid \boldsymbol{\Omega})\pi(\boldsymbol{\Omega}). \tag{28}$$

However, it is easy to see that (28) does not have a closed form. Besides, the marginal posterior of $\mathbf{Z}$ is intractable and it is therefore necessary to use MCMC algorithms, as we will see next. Recalling that one of our primary goals is to estimate Z_js, thus, the Bayes estimator of $\mathbf{Z}$ is given by

$$\hat{\mathbf{Z}}^{Bayes} = \sum_{i=1}^{L} \frac{\mathbf{Z}^{(i)}}{L}, \tag{29}$$

where $\mathbf{Z}^{(i)}$ is the i-th iteration and L is the total number of iterations of the MCMC chain. For the sake of space, see Appendix A for the relevant derivations of our novel computational strategy for the hybrid MCMC algorithm, as well as the supplementary material.

4. Simulation study

In this section, a simulation study is performed to evaluate the efficiency of the Bayesian estimators via the Monte Carlo method. To make our presentation easier, we consider two causes of failure with distinct parameters for each cause $\boldsymbol{\theta} = (\beta_1, \alpha_1, \beta_2, \alpha_2)$. The proposed simulation design is consistent with the following setup: (i) there are $m = (10, 50, 100)$ systems, each observed on the fixed time interval from $(0, 20]$; (ii) the failure process for each component follows a power-law NHPPs with intensity (9); (iii) among the many possible parameter choices, we provide details for ($\beta_1 = 1.2, \alpha_1 = 5, \beta_2 = 0.7, \alpha_2 = 13.33$) and ($\beta_1 = 0.75, \alpha_1 = 9.46, \beta_2 = 1.25, \alpha_2 = 12.69$); and (iv) we generate each random observation z_j, $j = 1, \ldots, m$, *iid* with mean one and variance η, according to a gamma distribution. In addition, we consider a set of values for variance of $\mathbf{Z}$, $\eta = (0.5, 1, 5)$, indicating low, middle and high dependence degrees, respectively. For each setup of parameters, we obtain the mean number of failures (5, 13.3), (9.5, 12.7), respectively. In the first simulated scenario, the mean number of failures of one of the components is predominant over the other component. In the last scenario, the mean number of failures of each component are almost equal to each other. It is worth noting that the obtained results are similar for other parameter combinations and can be extended to more causes, i.e. $p > 2$. Using the fact that the causes are dependent due to frailty term Z_j and also using the known results from the literature about NHPPs, in each Monte Carlo replication the failure times and indicators of the cause of failure were generated as shown in the following algorithm.

1: Generate iid $z_j \sim \gamma(\eta, 1/\eta)$ for $j = 1, 2, \ldots, m$, with mean one and variance η.

2: For each cause of failure, generate random numbers n_{j1} and n_{j2}, $j = 1, \ldots, m$, both from a Poisson distribution with mean $z_j \alpha_q$, for $q = 1, 2$, respectively.

3: For the q-th cause of failure from j-th system, let the failure times be $t_{j,1,q}, \ldots, t_{j,n_j,q}$, where $t_{j,i,q} = T\, U_{j,i,q}^{1/\beta_{jq}}$ and $U_{j,1,q}, \ldots, U_{j,n_j,q}$ are the order statistics of a size n_j random sample from the standard uniform distribution.

4: Finally, to obtain the data in the form (t_i, δ_i), let the t_is be the set of ordered failure times and set δ_i equal to j according to the corresponding cause of failure (i.e., set $\delta_i = 1$ if $t_i = t_{h,1}$ for some h or $\delta_i = j$ depending on the cause of failure).

Software R was used to implement this simulation study [27]. We considered two criteria to evaluate the estimators' behaviour: the Bias, given by $\text{Bias}_{\hat{\theta}_i} = \sum_{j=1}^{M}(\hat{\theta}_{i,j} - \theta_i)/M$ and the MSE, given by $\text{MSE}_{\hat{\theta}_i} = \sum_{j=1}^{M}(\hat{\theta}_{i,j} - \theta_i)^2/M$, where M is the number of estimates (i.e. the Monte Carlo size), where we take $M = 50,000$ throughout the section, and $\boldsymbol{\theta} = (\theta_1, \ldots, \theta_p)$ is the vector of parameters. Additionally, we computed the $CP_{95\%}$. Good estimators should have Bias, MSE close to zero and adequate intervals should be short while showing $CP_{95\%}$ close to 0.95. It is worth mentioning that the coverage probability of confidence interval is a frequentist concept. In Bayesian inference, the parameter always falls within the interval with the given probability such as 95%. The Bias and MSE are widely used to measure the performance evaluation.

The Bayes estimators for β_j and α_j were obtained using independent marginal posteriors according to gamma distributions given in (17). Since the marginal posterior distributions for the parameters β_j and α_j follow gamma distributions, we can obtain closed-form expressions for the posterior means and obtain the credibility intervals based on the 2.5% and 97.5% percentile posteriors. Hence, no MCMC was needed to obtain the estimates for these parameters. On the other hand, to obtain the estimates of the Z_js, $j = 1, \ldots, m$, we considered the HMC described in Appendix A. For each simulated data set, $10,000$ iterations were performed using the MCMC methods. As a burn-in, the first $5,000$ initial values were discarded. The Geweke criterion [28] was considered to check the convergence of the obtained chains under a 95% confidence level. In addition, trace and autocorrelation plots of the generated sampled values of each Z_j showed that they converged to the target distribution. The remaining $5,000$ were used for posterior inference. Specifically, these values were used to compute the posterior means of Z_js. Table 1 presents the Bias, the MSE and coverage probability with a 95% confidence level of the Bayes estimates for $\alpha_1, \alpha_2, \beta_1, \beta_2$ and the variance of Z.

As shown in Tables 1 and 2, the biases of the Bayes estimator are very close to zero for all the parameters, while both Bias and MSE tend to zero as m increases. Hence, in terms of Bias and MSE, the Bayes estimators provided accurate inferences for the parameters of the PLP model. In terms of coverage probabilities, we observed that using our Bayes estimators returned accurate credibility intervals even for a small number of system m. This result may be explained by the fact that our proposed Bayes estimators do not depend on asymptotic results to obtain the credibility intervals, which leads to accurate results for small sample sizes.

5. Application to the warranty repair data

The dataset considered in this section comprises the recurrent failure history of a fleet of identical automobiles obtained from

Table 1: The Bias, MSE, CP(95%) from the estimates considering different values for variance of Z and number of systems (m) with scenario $\boldsymbol{\theta}$=(1.2, 5, 0.7, 13.3).

η	Parameter	m	α_1	α_2	β_1	β_2	η
0.5	Bias	10	-0.0041	0.0083	-0.0001	0.0007	0.0784
		50	0.0011	-0.0055	-0.0001	0.0002	0.0276
		100	-0.0001	0.0074	0.0000	-0.0001	0.0165
	MSE	10	0.7035	1.1696	0.0729	0.0882	0.2709
		50	0.3182	0.5093	0.0321	0.0390	0.1359
		100	0.2230	0.3650	0.0225	0.0276	0.0957
	CP(95%)	10	0.9427	0.9443	0.9449	0.9501	0.8395
		50	0.9483	0.9500	0.9459	0.9506	0.9366
		100	0.9502	0.9496	0.9512	0.9488	0.9444
1	Bias	10	0.0084	-0.0105	0.0003	-0.0023	0.0307
		50	0.0020	-0.0007	-0.0006	0.0001	0.0253
		100	0.0010	0.0039	0.0000	0.0000	0.0158
	MSE	10	0.6996	1.1449	0.0735	0.0879	0.5395
		50	0.3120	0.5185	0.0316	0.0393	0.2891
		100	0.2231	0.3690	0.0226	0.0275	0.2015
	CP(95%)	10	0.9444	0.9517	0.9432	0.9477	0.9423
		50	0.9532	0.9488	0.9477	0.9477	0.9544
		100	0.9477	0.9472	0.9489	0.9492	0.9478
5	Bias	10	0.0174	-0.0120	-0.0005	0.0009	-0.1693
		50	-0.0017	-0.0085	-0.0009	0.0000	0.0453
		100	0.0000	0.0005	0.0001	-0.0004	-0.0425
	MSE	10	0.7156	1.1508	0.0723	0.0873	2.2234
		50	0.3179	0.5141	0.0317	0.0390	2.1358
		100	0.2239	0.3711	0.0223	0.0276	1.5038
	CP(95%)	10	0.9419	0.9508	0.9460	0.9483	0.9340
		50	0.9476	0.9504	0.9500	0.9472	0.9473
		100	0.9470	0.9462	0.9505	0.9476	0.9426

a warranty claim database presented in [1]. For the sake of clarity, our graphics present only the cars that presented failures in the observation period. Figure 1 shows the recurrence of failures of the 172 cars according to the cause of failure and the car mileage at each failure. The x-axis indicates the mileage. It is worth noting that the process of data collection has truncated time, where the observation period is 3000 miles for all cars. Each car from the fleet is represented by a horizontal line, where the cause of failure 1 is identified by the green circle, the cause of failure 2 by the red triangle and the cause of failure 3 by the blue square.

The main authors make only a table available (omitted here) containing the mileage to repeated failures of 172 vehicles, as well as the associated cause of failure. There were 76 failures related to the cause of failure 1, 87 related to the cause of failure 2 and 111 related to the cause of failure 3. They also pointed out that there were 267 cars that did not fail during the observation period. However, following the correct methodology, we consider 439 automobiles in our analysis.

In order to check the fit of the PLP model, the Duane plot is initially considered. Duane [29] popularized the standard application of such an approach by examining the time data between failures of various industrial systems, in which he observed that the cumulative rate of empirical failure normally produced a linear relationship with the accumulated operating

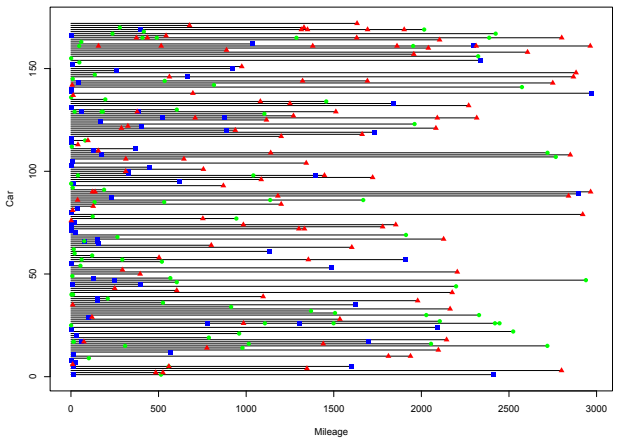

Figure 1: Recurrences of three causes of failure for 172 cars from warranty claims data. The green circle represents the cause of failure 1, the red triangle represents the cause of failure 2 and the blue square represents the cause of failure 3.

time when plotted on a log-log scale. Under the competitive risk approach and following [1; 30], we assessed the fit of the PLP for each cause of failure using the Duane plot. Figure 2 shows plots of logarithm of the number of failures $N_q(t)$ (for

Table 2: The Bias, MSE, CP(95%) from the estimates considering different values for variance of Z and number of systems (m) with scenario $\boldsymbol{\theta}$=(0.75, 9.5, 1.25, 12.7)

η	Parameter	m	α_1	α_2	β_1	β_2	η
0.5	Bias	10	0.0215	-0.0189	0.0004	0.0000	0.0745
		50	0.0017	-0.0003	0.0004	-0.0004	0.0218
		100	0.0025	-0.0005	0.0003	0.0001	0.0155
	MSE	10	0.9632	1.1248	0.0787	0.1120	0.2691
		50	0.4341	0.4992	0.0347	0.0495	0.1312
		100	0.3085	0.3569	0.0243	0.0350	0.0946
	CP(95%)	10	0.9498	0.9477	0.9467	0.9470	0.8346
		50	0.9506	0.9516	0.9497	0.9508	0.9377
		100	0.9471	0.9462	0.9509	0.9482	0.9417
1	Bias	10	-0.0025	-0.0013	0.0003	0.0003	0.0233
		50	0.0005	0.0039	-0.0004	0.0003	0.0155
		100	0.0024	-0.0013	0.0001	-0.0003	0.0087
	MSE	10	0.9678	1.1311	0.0780	0.1138	0.5279
		50	0.4340	0.5065	0.0346	0.0497	0.2808
		100	0.3087	0.3592	0.0246	0.0355	0.1987
	CP(95%)	10	0.9497	0.9503	0.9478	0.9471	0.9407
		50	0.9495	0.9465	0.9477	0.9515	0.9510
		100	0.9456	0.9470	0.9463	0.9482	0.9495
5	Bias	10	-0.0148	-0.0076	-0.0008	-0.0002	-0.1558
		50	-0.0027	-0.0039	0.0007	-0.0001	0.0577
		100	0.0040	-0.0040	-0.0003	0.0002	-0.1141
	MSE	10	0.9663	1.1197	0.0785	0.1119	2.2178
		50	0.4366	0.5044	0.0348	0.0497	2.0724
		100	0.3075	0.3592	0.0246	0.0347	1.4197
	CP(95%)	10	0.9517	0.9512	0.9493	0.9491	0.9354
		50	0.9491	0.9471	0.9499	0.9522	0.9479
		100	0.9489	0.9467	0.9497	0.9551	0.9485

$q = 1, 2, 3$) against the logarithm of the accumulated mileage at failure. Since the three plots exhibit reasonable linearity, the PLP model seems to be adequate.

In addition, to confirm the adequacy found in the visual inspection, we apply two statistical trend tests (goodness-of-fit tests): Cramer-von Mises and Lewis-Robison. For a detailed discussion of this point we refer the reader to [31], [32] and [33]. Following the arguments of [33], the tests here assume that the null hypothesis is a renewal process. Further, the tests were implemented considering the time truncated case (the R code for such tests can be found within the Supplementary Material). Based on these assumptions, the Cramer-von Mises statistic for the cause of failure 1 was 2.841, and the Lewis-Robison statistic was -5.246 both with $p < 0.0001$, so both lead to rejection of the null hypothesis. Cause of failure 2, the Cramer-von Mises statistic was 2.301, and the Lewis-Robison statistic was -4.706, both with $p < 0.0001$, then the null hypothesis in both tests is rejected. Finally, for the cause of failure 3, the Cramer-von Mises statistic was 0.623 giving $p = 0.0196$, and the Lewis-Robison statistic was -2.49 with $p = 0.01279$, again we have the same conclusions as to the previous ones. Therefore, we assume that PLPs govern the failure processes of all causes.

Based on this, we consider our proposed approach to fit the data. As presented in Section 3, we assume the prior distribution (16) for parameters α_q and β_q ($q = 1, 2, 3$) and, consequently, the marginal posterior distributions (17). On the basis of the latter consideration, the posterior mean estimates are computed in closed-form and the CIs are obtained directly from the gamma distribution. The results of the analysis are presented in Table 3, which show Bayes estimates along with the corresponding SDs and CIs. According to these data, the estimates of the shape parameters $\left(\hat{\beta}_1, \hat{\beta}_2, \hat{\beta}_3\right)$ are smaller than 1; see Table 3. This clearly indicates improvement in reliability.

Table 3: Parameter estimates for warranty claim dataset

Parameter	Bayes	SD	CI (95%)
β_1	0.300	0.035	[0.236 ; 0.372]
β_2	0.409	0.044	[0.327 ; 0.500]
β_3	0.698	0.067	[0.574 ; 0.835]
α_1	0.173	0.020	[0.136 ; 0.214]
α_2	0.198	0.021	[0.159 ; 0.242]
α_3	0.253	0.024	[0.208 ; 0.302]
$Var(Z)$	1.755	0.438	[1.050 ; 2.777]

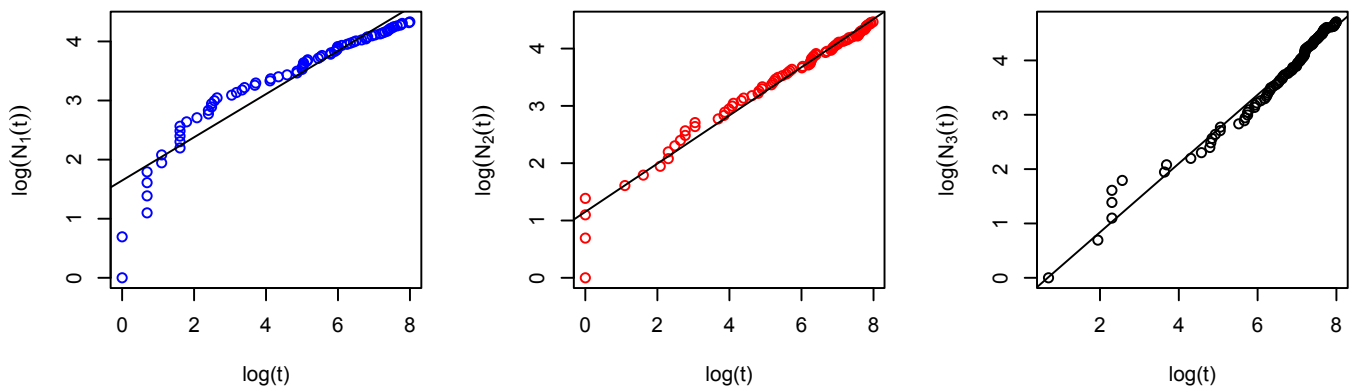

Figure 2: The plot shows a fairly linear pattern for the three causes of failure indicating the fit according to the PLP model: cause 1 (blue circles); cause 2 (red circles) and cause 3 (black circles)

The hybrid MCMC sampler algorithm presented in Section 6 was used to obtain a sample from the joint posterior distribution related to the frailty distribution. The initial values to start the sample of the chains for the DPM were random. For the MCMC chain, we considered 10,000 iterations initially, where the first 5,000 were discarded as burn-in samples and the last 5,000 iterations were used to compute the posterior estimates of $Var(Z)$ (at the bottom of the Table 3) and the individual values of Z_js, as presented in Figure 3. The convergence was monitored for the Geweke test assuming a 95% confidence level (see Figure 6 in Appendix A). For completeness, we also present MCMC diagnostic plots, such as traces and autocorrelations for the HMC algorithm; see Appendix B.

It is worth pointing out that higher values of $Var(Z)$ signify greater heterogeneity among systems and more dependence between the times of the causes of failure for the same system. Therefore, as Table 3 shows, the posterior mean of $Var(Z)$ provides evidence of a meaningful dependence between the times of the causes of failure within a system.

5.1. Insights on the unobserved heterogeneity

As shown in Table 3, the estimate of $Var(Z)$ shows that there is strong posterior evidence of a meaningful degree of heterogeneity in the population of systems. Table 4 (Appendix B) shows the estimated posterior means and the corresponding standard deviations of the $\hat{z}_j$s.

Figure 3 shows the individual frailty estimates (posterior means) of $\hat{z}_j$, $j = 1, \ldots, 172$. As mentioned earlier, each Z_j acts in a multiplicative way in the specific-cause intensities. Thus it follows that values of Z_j equal to or very close to 1 (red line) do not significantly affect such intensities. On the other hand, values larger than 1 indicate increased intensity. It is apparent that some cars have values of Z_j greater than 2. These cars are probably subject to environmental stress variations or other unobserved issues, which make them more vulnerable than those with Z_j values closer to or less than 1.

Figure 4 indicates that the estimated frailties are overall larger for cars that had a failure early than those who had a failure later. We also note that a system with a large value of $\hat{z}_j$ experienced more failures than a system with a smaller value of $\hat{z}_j$ (see Figure 5).

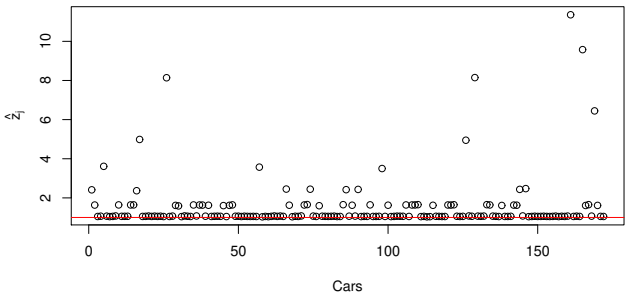

Figure 3: The individual frailty estimates, $\hat{z}_j$'s. The red line highlights value 1 in the y-axis.

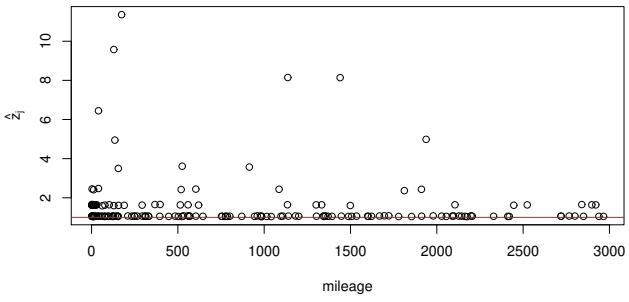

Figure 4: Estimated frailty versus mileage observed at failure for each car in automobile warranty data. The red line highlights value 1 in the y-axis. The reasoning is that cars that are more frail failed earlier than ones that are less frail.

These outcomes indicate that neglecting these effects can result in an underestimation of the parameters. Overall, the multiplicative shared frailty model is appropriate for modeling this effect accurately.

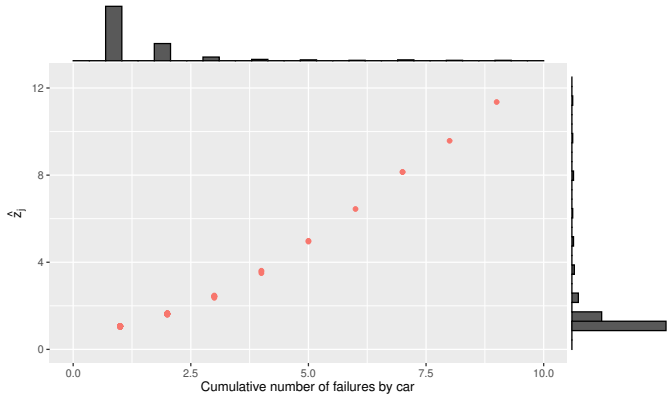

Figure 5: Scatterplot of individual estimates $\hat{z}_j$ against cumulative number of failures by car. Note that systems with a large value of $\hat{z}_j$ experienced more failures than a system with a smaller value of $\hat{z}_j$.

6. Conclusions

In this work, we proposed a new approach to analyzing multiple repairable systems data under the action of dependent competing risks. We have shown how to model the frailty-induced dependence nonparametrically using a DPM which does not make restrictive assumptions about the density of the frailty variable. Regarding PLP parameters, we propose a class of noninformative priors whose resulting posterior distributions are proper and we obtain closed-form Bayesian estimators. Although some research has been carried out on nonparametric frailty in the reliability field [14; 15], to the best of our knowledge, the proposed approach is the first for this competing risks setup.

The main focus of this work was to analyzing multiple repairable systems data under the action of dependent competing risks. An orthogonal parametrization for the cause-specific intensity PLP parameters was presented, which allowed us to consider a generalized version of [22] prior distribution for the parameters of the model. We provide estimates for the PLP model taking into account the dependence effect among component failures of the system. Such a dependence effect influences the statistical inferences of the model parameters, thus the misspecification of the frailty distribution may lead to errors when estimating the quantities of interest. We considered a Bayesian nonparametric prior to describing the frailty distribution due to its flexibility in modeling unknown distributions. Also, we proposed a hybrid MCMC algorithm that comprises a mixture of the Gibbs sampler and the HMC method, thus generating a chain with little dependence. Although some research has been carried out on nonparametric frailty in the reliability field [14; 15], to the best of our knowledge, the proposed approach is the first for this competing risks setup. Our proposed approach to these problems is fully Bayesian and is advantageous because we can perform an individual posterior analysis of the quantities of interest, i.e., we estimate the interest parameters of the PLP (our main focus) separately from nuisance parameter of frailty distribution (variance).

A simulation study was conducted to confirm our theoretical results, as well as to measure if the variability of the frailty distributions was correctly computed. This study returned excellent results that confirmed that our Bayes estimators are robust in terms of Bias, MSE and coverage probabilities. we can obtain more precise parameter estimations by considering the high flexibility due to nonparametric Bayesian prior density for Z. It also enables us to obtain insights into the heterogeneity between the systems by individually estimating Z_js, as presented in Section 5.1. The proposed approach was implemented in statistical software that can be easily used to obtain the estimates and to conduct the analysis.

There are many possible extensions of our current work, more flexible modeling can be further proposed by extending our approach to model the intensity function of failures of the NHPP nonparametrically since that the PLP intensity cannot capture non-monotonic behaviors. This extension would make the model more robust and flexible. In this case, we would have a fully nonparametric approach. Here, our proposed study focus on a reparable system under minimal repair, on the other hand, a similar study can also be further adapted under other types of repair such as perfect or imperfect [34; 35]. Identifying the significant covariates which affect the failure process is also of the main interesting and this approach should also be investigated in the presence of covariates.

Finally, our method can be further extended for other models with additional complexity such as a hierarchical structure [36]. Our approach should be investigated further in these contexts.

SUPPLEMENTARY MATERIAL

The zip file NPB.zip contains the C++ codes (NPB25.cpp and rgig.cpp) for hybrid MCMC algorithm; It also contains the warranty data (cdcars.csv) used in our analysis (Section 5) and the R codes (appdataset.R) for generating the results of the referred analysis, as well as for the trend tests for adequacy of PLPs (gof.R).

Acknowledgment

The authors are very grateful to the Editor and the reviewer for their helpful and useful comments that improved the manuscript. Pedro L. Ramos is grateful to the São Paulo State Research Foundation (FAPESP Proc. 2017/25971-0). Francisco Louzada is supported by the Brazilian agencies CNPq (grant number 301976/2017-1) and FAPESP (grant number 2013/07375-0).

References

[1] A. Somboonsavatdee, A. Sen, Parametric inference for multiple repairable systems under dependent competing risks, Applied Stochastic Models in Business and Industry 31 (5) (2015) 706–720.

[2] N. Zhang, Q. Yang, Optimal maintenance planning for repairable multi-component systems subject to dependent competing risks, IIE Transactions 47 (5) (2015) 521–532.

[3] M. Wu, Y. Shi, C. Zhang, Statistical analysis of dependent competing risks model in accelerated life testing under progressively hybrid censoring using copula function, Communications in Statistics-Simulation and Computation 46 (5) (2017) 4004–4017.

[4] X. Zhang, A. Wilson, System reliability and component importance under dependence: A copula approach, Technometrics 59 (2) (2017) 215–224.
[5] W. Peng, L. Shen, Y. Shen, Q. Sun, Reliability analysis of repairable systems with recurrent misuse-induced failures and normal-operation failures, Reliability engineering & system safety 171 (2018) 87–98.
[6] X. Liu, Planning of accelerated life tests with dependent failure modes based on a gamma frailty model, Technometrics 54 (4) (2012) 398–409.
[7] J. Sethuraman, A constructive definition of dirichlet priors, Statistica sinica (1994) 639–650.
[8] M. Kalli, J. E. Griffin, S. G. Walker, Slice sampling mixture models, Statistics and computing 21 (1) (2011) 93–105.
[9] A. F. Smith, G. O. Roberts, Bayesian computation via the gibbs sampler and related markov chain monte carlo methods, Journal of the Royal Statistical Society: Series B (Methodological) 55 (1) (1993) 3–23.
[10] R. M. Neal, et al., Mcmc using hamiltonian dynamics, Handbook of Markov Chain Monte Carlo 2 (11) (2011) 2.
[11] J.-M. Hu, H.-Z. Huang, Y.-F. Li, Reliability growth planning based on information gap decision theory, Mechanical Systems and Signal Processing 133 (2019) 106274.
[12] J. Liu, L. Huang, R. Zhou, M. Volmer, Reliability growth test planning and verification of commercial vehicles, Automotive Innovation 2 (4) (2019) 328–337.
[13] R. C. P. dos Reis, E. A. Colosimo, G. L. Gilardoni, et al., Hierarchical modelling of power law processes for the analysis of repairable systems with different truncation times: An empirical bayes approach, Brazilian Journal of Probability and Statistics 33 (2) (2019) 374–396.
[14] V. Slimacek, B. H. Lindqvist, Nonhomogeneous poisson process with nonparametric frailty, Reliability Engineering & System Safety 149 (2016) 14–23.
[15] V. Slimacek, B. H. Lindqvist, Nonhomogeneous poisson process with nonparametric frailty and covariates, Reliability Engineering & System Safety 167 (2017) 75–83.
[16] D. R. Cox, N. Reid, Parameter orthogonality and approximate conditional inference, Journal of the Royal Statistical Society. Series B (Methodological) (1987) 1–39.
[17] P. Hougaard, Analysis of multivariate survival data, Springer Science & Business Media, 2012.
[18] P. K. Andersen, O. Borgan, R. D. Gill, N. Keiding, Statistical models based on counting processes, Springer Science & Business Media, 2012.
[19] S. E. Rigdon, A. P. Basu, Statistical methods for the reliability of repairable systems, Wiley New York, 2000.
[20] J. H. Cha, M. Finkelstein, Some notes on unobserved parameters (frailties) in reliability modeling, Reliability Engineering & System Safety 123 (2014) 99–103.
[21] Z. G. Asfaw, B. H. Lindqvist, Unobserved heterogeneity in the power law nonhomogeneous poisson process, Reliability Engineering & System Safety 134 (2015) 59–65.
[22] S. K. Bar-Lev, I. Lavi, B. Reiser, Bayesian inference for the power law process, Annals of the Institute of Statistical Mathematics 44 (4) (1992) 623–639.
[23] R. E. Kass, L. Wasserman, The selection of prior distributions by formal rules, Journal of the American Statistical Association 91 (435) (1996) 1343–1370.
[24] D. D. Dey, P. Müller, D. Sinha, Practical nonparametric and semiparametric Bayesian statistics, Vol. 133, Springer Science & Business Media, 2012.
[25] C. E. Antoniak, Mixtures of dirichlet processes with applications to bayesian nonparametric problems, The annals of statistics (1974) 1152–1174.
[26] M. D. Escobar, M. West, Bayesian density estimation and inference using mixtures, Journal of the american statistical association 90 (430) (1995) 577–588.
[27] R Core Team, R: A Language and Environment for Statistical Computing, R Foundation for Statistical Computing, Vienna, Austria (2016).
URL `https://www.R-project.org`
[28] J. Geweke, Evaluating the accuracy of sampling-based approaches to the calculations of posterior moments, Bayesian statistics 4 (1992) 641–649.
[29] J. Duane, Learning curve approach to reliability monitoring, IEEE transactions on Aerospace 2 (2) (1964) 563–566.
[30] A. Somboonsavatdee, A. Sen, Statistical inference for power-law process with competing risks, Technometrics 57 (1) (2015) 112–122.
[31] J. F. Lawless, C. Çiğşar, R. J. Cook, Testing for monotone trend in recurrent event processes, Technometrics 54 (2) (2012) 147–158.
[32] R. Cook, J. Lawless, Concepts and tests for trend in recurrent event processes (2013).
[33] J. T. Kvaløy, B. H. Lindqvist, A class of tests for trend in time censored recurrent event data, Technometrics 62 (1) (2020) 101–115.
[34] I. Nafisah, M. Shrahili, N. Alotaibi, P. Scarf, Virtual series-system models of imperfect repair, Reliability Engineering & System Safety 188 (2019) 604–613.
[35] A. Syamsundar, V. Naikan, V. Couallier, Accelerated failure time models with corrective and preventive maintenance for repairable systems, Reliability, Safety and Hazard Assessment for Risk-Based Technologies: Proceedings of ICRESH 2019 (2019) 143.
[36] F. Louzada, J. A. Cuminato, O. M. Rodriguez, V. L. Tomazella, P. H. Ferreira, P. L. Ramos, S. R. Niaki, O. A. Gonzatto, I. C. Perissini, L. F. Alegría, et al., A repairable system subjected to hierarchical competing risks: Modeling and applications, IEEE Access 7 (2019) 171707–171723.
[37] D. Eddelbuettel, C. Sanderson, Rcpparmadillo: Accelerating r with high-performance c++ linear algebra, Computational Statistics and Data Analysis 71 (2014) 1054–1063.
URL `http://dx.doi.org/10.1016/j.csda.2013.02.005`

Appendix A - MCMC algorithm

This Appendix describes an MCMC algorithm to sample from the posterior distribution of Z. Our algorithm is based on Kalli et al. [8], and its main characteristic is to estimate infinite parameters by introducing latent variables. We introduce a finite set of latent variables with uniform distribution with parameters 0 and 1, denoted by $U \sim \text{Uniform}[0, 1]$. Therefore, applying the variable U in (23) follows the joint density of (Z, U)

$$f_{Z,U}(z, u \mid \boldsymbol{\Omega}) = \sum_{l=1}^{\infty} \mathcal{LN}(z \mid \mu_l, \tau_l^{-1}) \mathbb{I}(u < \rho_l), \tag{30}$$

where $\mathbb{I}(\cdot)$ is an indicator function. Note that there is a finite number of elements in $\boldsymbol{\rho}$ which are greater than u, denoted as $A_{\boldsymbol{\rho}}(u) = \{j : \rho_j > u\}$. Therefore, the representation in (30) is similar to

$$f_{Z,U}(z, u \mid \boldsymbol{\Omega}) = \sum_{l \in A_\rho} \mathcal{LN}(z \mid \mu_l, \tau_l^{-1}), \tag{31}$$

so that, given $\mathbf{U}$, the number of mixture components is finite for $\mathbf{Z}$.

In order to simplify the likelihood, we introduce a new discrete latent variable Y which indicates the mixture component that Z comes from

$$f_{Z,U,Y}(z, u, Y = l \mid \boldsymbol{\Omega}) = \mathcal{LN}(z \mid \mu_l, \tau_l^{-1}) \mathbb{I}(l \in A_{\boldsymbol{\rho}}(u)). \tag{32}$$

Note that $Pr(Y = l \mid \boldsymbol{\Omega}) = \rho_l$, $\forall l = 1, 2, \ldots$, therefore the conditional distribution of $Z \mid U, Y = l$ is log-normal with parameters μ_l and τ_l^{-1}, so $W \mid U, Y = l \sim \mathcal{N}(\mu_l, \tau_l^{-1})$. Hence, the complete posterior distribution of $\mathbf{Z}, \boldsymbol{\Omega}$ with the latent variables $\mathbf{U}$ and $\mathbf{Y}$ is given by

$$\begin{aligned} \pi(\mathbf{Z}, \boldsymbol{\Omega}, \mathbf{U}, \mathbf{Y} \mid \mathbf{D}) \propto L_1(\mathbf{Z}|\mathbf{D}) f_{Z,U,Y}(\mathbf{Z} \mid \boldsymbol{\Omega}, \boldsymbol{U}, \boldsymbol{Y}) f_U(\boldsymbol{U}) \\ \times Pr(\boldsymbol{Y} \mid \boldsymbol{\Omega}) \pi(\boldsymbol{\Omega}), \end{aligned} \tag{33}$$

where $\boldsymbol{U} = \{U_j\}_{j=1}^m$ and $\boldsymbol{Y} = \{Y_j\}_{j=1}^m$ are latent variables.

Hybrid MCMC - computational strategy

Using the latent variables presented above, we now construct the following MCMC algorithm which is a combination of the Gibbs sampler with the HMC method. For more details on the HMC method, see Neal et al. [10]. We chose the HMC algorithm because it generates samples with less dependence with a high probability of acceptance between state if compared with the Random Walk Metropolis-Hastings algorithm. The Gibbs algorithm requires knowledge of complete conditional distributions in order to be able to sample from them. For further details, see [8] and [26]. The complete conditional distributions are listed below.

1. **Conditional Distribution of c**

   Escobar and West [26] shows that given $\mathbf{Y}$, the parameter is independent of all other parameters and the conditional distribution of c is given by

$$\pi(c \mid \mathbf{Y}) \propto (c+m)c^{y^*-1}\mathcal{G}(c \mid ac_0, bc_0)\,\mathbb{B}(c+1,m) \times \mathbb{I}(c>0), \tag{34}$$

   where $y^* = \max(\mathbf{Y})$ and $\mathbb{B}(\cdot,\cdot)$ is the Beta function. Using the definition of the Beta function we can create an auxiliary variable ξ with the joint distribution for which the marginal distribution is (34) and is given by

$$\pi(c,\xi \mid \mathbf{Y}) \propto (c+m)c^{y^*-1}\xi\mathcal{G}(c \mid ac_0, bc_0) \times \xi^c(1-\xi)^{m-1}\,\mathbb{I}(c>0)\mathbb{I}(0<\xi<1). \tag{35}$$

   Hence, it follows that the conditional posteriors of ξ and c are given by

$$\xi \mid c, \mathbf{Y} \sim \mathcal{B}(c+1, m) \tag{36}$$

   and

$$c \mid \xi, \mathbf{Y} \sim p_\xi \mathcal{G}(a_1^*, b_1^*) + (1-p_\xi)\mathcal{G}(a_2^*, b_1^*), \tag{37}$$

   where $a_1^* = a_0 + y^*$, $a_2^* = a_1^* + 1$, $b_1^* = b_0 - \log(\xi)$ and $p_\xi = (a_0 + y^* - 1)/(a_0 + z^* - 1 + m(b_0 - \log(\xi))$. Therefore, c can be sampled using the auxiliary ξ with equations (36) and (37).

2. **Conditional Distribution of ν**

   Note that by equations (32) and (33), ν depends on $\mathbf{Y}$, $\mathbf{U}$ and c, therefore the conditional distribution of ν is

$$\nu_l \mid \mathbf{Y}, \mathbf{U}, c \sim \begin{cases} \mathcal{B}(n_l+1, m+\sum_{o=1}^{l} n_o + c) & ,\forall l = 1,\ldots,y^* \\ \mathcal{B}(1,c) & ,\forall l = y^*+1, \\ & \quad y^*+2,\ldots, \end{cases} \tag{38}$$

   where n_l is the number of observations in the l-th component. It is worth noting that in order to sample $\boldsymbol{\rho}$ it is enough to simulate $\boldsymbol{\nu}$ calculated by equation (24).

3. **Conditional Distribution of U**

   The latent variable U depends only on $\boldsymbol{\rho}$, and the conditional distribution of $\mathbf{U}$ is

$$U_j \mid \boldsymbol{\rho} \sim \text{Uniform}[0, \rho_j]\ \forall j = 1,2,\ldots,m. \tag{39}$$

4. **Conditional Distribution of μ and τ**

   The μ and τ parameters of each component are independent and adding the fact that the Normal-Gamma is conjugated from the Normal distribution, the conditional distribution of $\boldsymbol{\mu}$ and $\boldsymbol{\tau}$ is given by

$$\mu_l, \tau_l \mid \mathbf{Y} \sim \begin{cases} \mathcal{NG}(m_l, s_l, d_l p_l, d_l) & ,\forall l = 1,\ldots,y^* \\ \mathcal{NG}(m_0, s_0, d_0 p_0, d_0) & ,\forall l = y^*+1, y^*+2,\ldots, \end{cases} \tag{40}$$

   where

$$\begin{aligned} m_l &= \frac{s_0 m_0 + n_l \bar{w}}{s_0 + n_l}, \\ s_l &= s_0 + n_l, \\ d_l p_l &= d_0 p_0 + \sum_{j:y_j=l}(w_j - \bar{w})^2 + \frac{s_0 n_l}{s_0+n_l}(m_0 - \bar{w})^2, \\ d_l &= d_0 + n_l, \\ \bar{w} &= \sum_{j:y_j=l} \frac{w_j}{n_l}. \end{aligned}$$

5. **Conditional Distribution of Y**

   The latent variable Y is discrete, therefore using equations (32) and (33) the conditional distribution of $\mathbf{Y}$ is

$$Pr(Y_j = l \mid \boldsymbol{\Omega}, \mathbf{W}, \mathbf{U}, \mathbf{D}) \propto \mathcal{N}(w \mid \mu_l, \tau_l^{-1})\mathbb{I}(l \in A_\rho). \tag{41}$$

6. **Conditional Distribution of Z**

   The conditional distribution of $\mathbf{Z}$ is given by

$$\pi(\mathbf{Z} \mid \boldsymbol{\Omega}, \boldsymbol{U}, \boldsymbol{Y}, \boldsymbol{D}) \propto \prod_{j=1}^{m} \mathcal{LN}(z_j \mid \mu_{Y_j}, \tau_{Y_j}^{-1}) L_1(\mathbf{Z}|\mathbf{D}), \tag{42}$$

   with restriction $\bar{\mathbf{Z}} = 1$. Different from the previous parameters and latent variable, we simulate them using the HMC algorithm. However, the HMC algorithm requires that the support random variable is unrestricted. Therefore, we transform the variable $\mathbf{Z}$ to a variable with unrestricted support as explained below.

   Let $\mathbf{Z}^*$ be a random vector with $m-1$ elements and unrestricted support. We define the following variables:

$$\begin{aligned} B_j &= \text{logit}^{-1}(Z_j^* - \log(m-j)), \\ A_j &= \left(1 - \sum_{j'=1}^{j-1} A_{j'}\right) B_J \quad \forall j = 1,2,\ldots,m-1, \\ A_m &= 1 - \sum_{j'=1}^{m-1} A_{j'}, \end{aligned} \tag{43}$$

   where $logit^{-1}$ is an inverse function of *logit*. Note that the functions of transformed variables are bijection, $B_j \in (0,1)$ and $\text{sum}(\mathbf{A}) = 1$. Naturally, we assume that $\mathbf{Z} = m\mathbf{A}$. Therefore, the determinant of the Jacobian matrix is given by,

$$\mid J(\mathbf{z}^*) \mid = \prod_{j=1}^{m-1}\left(b_j(1-b_j)\left(1 - \sum_{j'=1}^{j-1} a_{j'}\right)\right).$$

   Therefore, the conditional distribution of $\mathbf{Z}^*$ is given by

$$\pi(\mathbf{Z}^* \mid \boldsymbol{\Omega}, \boldsymbol{U}, \boldsymbol{Y}, \boldsymbol{D}) \propto \mid J(\mathbf{z}^*) \mid \mathcal{LN}(z_j \mid \mu_{Y_j}, \tau_{Y_j}^{-1}) \times L_1(\mathbf{Z}|\mathbf{D}). \tag{44}$$

Thus, we constructed a Hybrid MCMC algorithm that combines Gibbs sampling with HMC sampling to sample $\mathbf{Z}$ and $\mathbf{\Omega}$; see algorithm below.

1: Initialize $c^{(0)}$, $\mathbf{Z}^{*(0)}$ and $\mathbf{Y}^{(0)}$.
2: Calculate $\mathbf{Z}^{(0)}$ of Equation (43) and $\mathbf{W}^{(0)} = \log(\mathbf{Z}^{(0)})$.
3: Draw $\xi^{(i)}$ from $\pi(\xi \mid c^{(i-1)}, \mathbf{Y}^{(i-1)})$ of Equation (36).
4: Draw $c^{(i)}$ from $\pi(c \mid \xi^{(i)}, \mathbf{Y}^{(i-1)})$ of Equation (37).
5: Draw $\nu_l^{(i)}$ from $\pi(\nu_l \mid \mathbf{Y}^{(i-1)}, c^{(i)})$ of Equation (38), $\forall l = 1, 2, \ldots, y^*$.
6: Calculate $\rho_l^{(i)}$ of Equation (24) $\forall l = 1, 2, \ldots, y^*$.
7: Draw $U_j^{(i)}$ from $\pi(U_j \mid \boldsymbol{\rho}^{(i)})$ of Equation (39) $\forall j = 1, 2, \ldots, m$.
8: Find the smallest l^* such that $\sum_{l=1}^{l^*} \rho_l > (1 - \min(\mathbf{U}^{(i)}))$ and draw $\nu_l^{(i)}$ from $\pi(\nu_l \mid \mathbf{Y}^{(i-1)}, c^{(i)})$, $\forall l = y^* + 1, \ldots, l^*$.
9: Draw $\mu_l^{(i)}$ and $\tau_l^{(i)}$ from $\pi(\mu_l, \tau_l \mid \mathbf{Y}^{(i-1)})$ of Equation (40) $\forall l = 1, 2, \ldots, l^*$.
10: Draw $Y_j^{(i)}$ from $Pr(Y_j \mid \boldsymbol{\mu}^{(i)}, \boldsymbol{\tau}^{(i)}, \mathbf{W}^{(i-1)}, \mathbf{U}^{(i)}, \mathbf{D})$ of Equation (41) $\forall j = 1, 2, \ldots, m$.
11: Draw $\mathbf{Z}^{*(i)}$ from $\pi(\mathbf{Z}^* \mid \boldsymbol{\mu}^{(i)}, \boldsymbol{\tau}^{(i)}, \boldsymbol{U}^{(i)}, \boldsymbol{Y}^{(i)})$ of Equation (44).
12: Calculate $\mathbf{Z}^{(i)}$ of Equation (43) and $\mathbf{W}^{(i)} = \log(\mathbf{Z}^{(i)})$.
13: Set $i = i + 1$ and go to Step #3.

In this scheme, the HMC sampler is applied in Step #11. The algorithm was developed in the C++ language using the RccpArmadilho library [37]. Its main advantages are processing speed and interaction with the R program [27]. This code was used both in the generation of posterior sampling and in the simulation study presented in the following section.

Appendix B

In this appendix, we presented estimates of some Z_j's associated to cars 1, 17, 26, 161, 165 and 169, according to Figure 3 (these are the estimates that presented the highest values). red For completeness, we also present here the Geweke diagnostic test for checking the convergence of the chains, as well as MCMC diagnostic plots, such as trace and autocorrelations for the HMC algorithm of some Z_js. In addition, we present the data structure, Table 5.

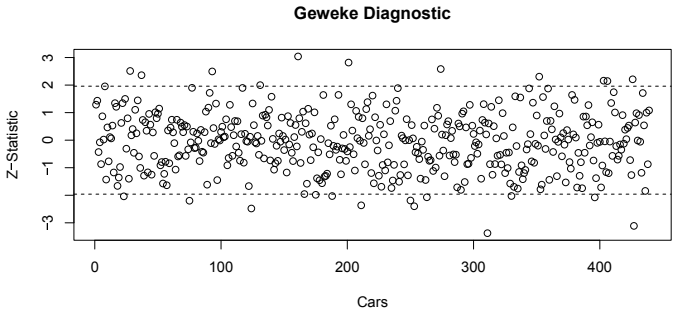

Figure 6: Geweke diagnostic test - implemented using CODA package in R software.

Table 4: Bayesian estimates of some Z_js with their SD.

Z_j	Bayes	SD
Z_1	2.469	1.711
Z_{17}	5.1	2.87
Z_{26}	8.269	3.669
Z_{161}	11.519	4.359
Z_{165}	9.941	4.038
Z_{169}	6.615	3.354

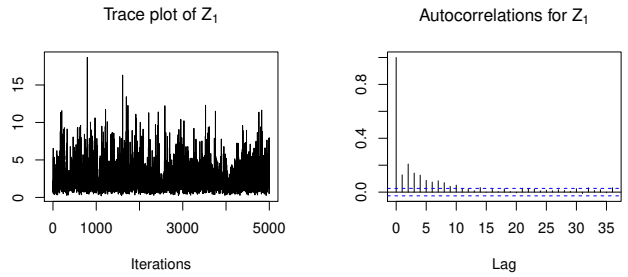

Figure 7: Markov chain and autocorrelation plots for the HMC algorithm - Z_1.

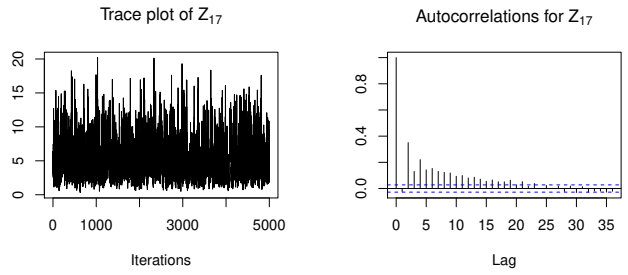

Figure 8: Markov chain and autocorrelation plots for the HMC algorithm - Z_{17}.

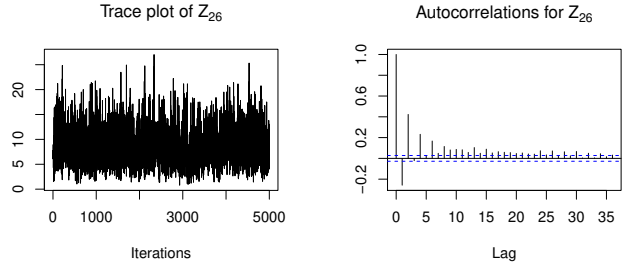

Figure 9: Markov chain and autocorrelation plots for the HMC algorithm - Z_{26}.

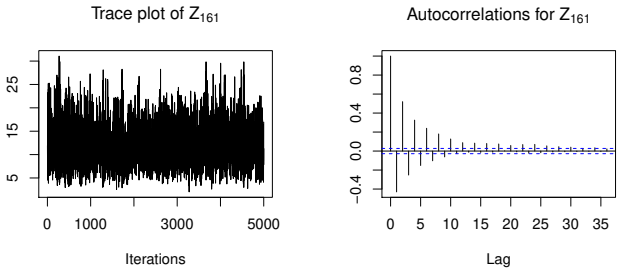

Figure 10: Markov chain and autocorrelation plots for the HMC algorithm - Z_{161}.

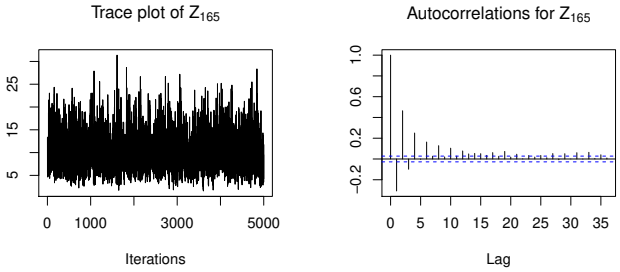

Figure 11: Markov chain and autocorrelation plots for the HMC algorithm - Z_{165}.

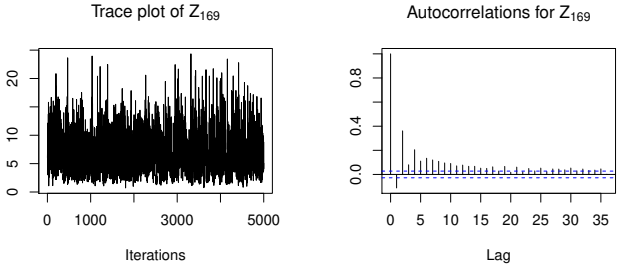

Figure 12: Markov chain and autocorrelation plots for the HMC algorithm - Z_{169}.

Table 5: Data structure - Observations for m systems with K competing risks.

System	Competing Risks (δ)	Failure times (t_{ji})	Number of failures (n_{jq})
	1	$t_{11}, t_{12}, \ldots, t_{1n_{11}}$	n_{11}
1	2	$t_{11}, t_{12}, \ldots, t_{1n_{12}}$	n_{12}
	$\vdots$	$\vdots$	$\vdots$
	K	$t_{11}, t_{12}, \ldots, t_{1n_{1K}}$	n_{1K}
	$\vdots$	$\vdots$	$\vdots$
$\vdots$	$\vdots$	$\vdots$	$\vdots$
	$\vdots$	$\vdots$	$\vdots$
	$\vdots$	$\vdots$	$\vdots$
	1	$t_{m1}, t_{m2}, \ldots, t_{mn_{m1}}$	n_{m1}
m	2	$t_{m1}, t_{m2}, \ldots, t_{mn_{m2}}$	n_{m2}
	$\vdots$	$\vdots$	$\vdots$
	K	$t_{m1}, t_{m2}, \ldots, t_{mn_{mK}}$	n_{mK}